INFLUENCE OF FLUID EMISSION THROUGH A PROFILE'S TRAILING EDGE ON THE BOUNDARY LAYER

Dan Scurtu[1], Doru Calarasu[1], Bogdan Ciobanu[1]& Oreste Vascan[2]

[1] "Gheorghe Asachi" Technical University of Iasi-Romania, Department of Fluid Mechanics, Blvd. Mangeron No. 67, 700050 Iasi, Romania
[2] Crescendo International SRL, Fecioarei Street, 13 Bucharest, Romania

Corresponding author: Dan Scurtu, scurtud@yahoo.com

Abstract The goal, for any airfoil placed in a real fluid flow, is to achieve the highest possible lifting capacity. A high lifting capacity means both a high lift coefficient and a low resistance coefficient.
The paper discusses a procedure meant to increase the lift coefficient and at the same time decrease the resistance coefficient. The procedure employed consists of launching through a profile's trailing edge a fluid jet of quantifiable outflow. The jet fluid has the same nature as the general flow fluid.
It describes the pressure variation evolution along the upper side of classical profile and fluid emission profile and it comprises the conclusions of the analysis of this evolution.
Key words: airfoil, lift coefficient, resistance coefficient, lifting capacity, fluid emission.

1. INTRODUCTION

The goal, for any airfoil placed in a real fluid flow, is to achieve the highest possible lifting capacity. The interaction between the real fluid flow and the airfoil outline triggers the occurrence of a lifting force F_L and of a resistance force F_D:

$$F_L = \frac{\rho}{2} \cdot b \cdot c \cdot C_L \cdot w_0^2$$
$$F_D = \frac{\rho}{2} \cdot b \cdot c \cdot C_D \cdot w_0^2 \qquad (1)$$

where: ρ [kg/m^3] is the fluid flow density, b [m] is the wing span, c [m] is the chord, w_0 [m/s] is the fluid flow speed, C_L is the lift coefficient, and C_D is the resistance coefficient.
The lifting capacity λ of the profile is defined:

$$\lambda = \frac{C_L}{C_D} \qquad (2)$$

A high lifting capacity means both a high C_L coefficient and a low C_D coefficient. The polar curve analysis performed on the catalogue profiles revealed that both C_L and C_D depend on the incidence α angle of the profile in the fluid flow: $C_D = C_D(\alpha)$, $C_L = C_L(\alpha)$. Please note that the alteration of the incidence angle designed to increase the C_L coefficient also increases the C_D coefficient.
In order to avoid this drawback, the paper proposes a procedure meant to increase the lift coefficient C_L and at the same time decrease the resistance coefficient C_D. [1], [5]

2. GENERAL INFORMATION

The procedure employed consists of launching through a profile's trailing edge a fluid jet of quantifiable outflow.
The jet fluid has the same nature as the general flow fluid.
The profile trailing edge fluid emission is assimilated to a plane source, compared to the profile span unit.
The cyclic motion theory may therefore be used for the mathematical modeling of the fluid motion.
The theoretical results obtained by fluid emission through the wing trailing edge were compared to those obtained on a classical wing.
A boundary layer occurs both in the classical wing and in the fluid emission wing, when they are placed in a real mobile fluid flow with a w_0 speed. This layer evolves at both the upper and lower wing side levels. It is the evolution of the boundary layer on the upper wing side that it is of the highest interest for us.
The whole effect of the friction forces generated by fluid viscosity is concentrated within the boundary layer.
Therefore, the fluid flow in the boundary layer area is described using the Karmann equations. Within the boundary layer, the fluid in motion is considered ideal and its motion is modeled by Euler equations.
The concept of boundary layer thickness δ [m] is employed to characterize the boundary layer. The maximum thickness that the boundary layer may reach is $\delta_{\max} = \delta(c) = 0,01 \cdot c$ where c is the profile chord.
In some cases, the boundary layer may follow the entire profile outline, which means that the

detachment occurs in the trailing edge area. In most cases however, the boundary layer detachment occurs at a point located between the leading edge and the trailing edge.

When the pressure gradient remains negative along the upper profile side, the boundary layer detachment occurs in the trailing edge.

If, however, there are certain areas on the upper side along the general motion direction, for which the pressure gradient becomes positive, then the boundary layer detachment also takes place in these areas.

The boundary layer fluid motion, which determines whether the pressure variation in the flow direction is positive or negative, is described by the local speed *u* [m/s], the local pressure *p* [N/m^2], the local thickness of the boundary layer δ [m] and the viscous friction coefficient in the boundary layer τ [N/m^2].[2], [3]

3. MATHEMATICAL MODEL

The theoretical study was performed on an airfoil built using an aerodynamic Gö593 profile (figure 1).

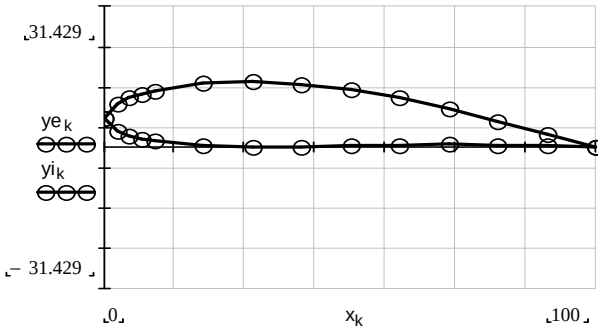

Fig. 1. Geoametry of Gö593 profile

The conformal transformation theory therefore applies when modeling the flow around the chosen profile. According to this theory, the profile outline suffers a biunique conversion, turning into the outline of a **K** circle with the radius $a = \frac{c}{4}$ (figure 2).

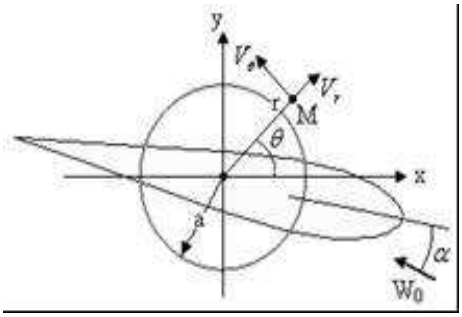

Fig. 2. Conformal transformation circle

The values of the transformation mapp functions in the x_i (i = 1÷17) points of the profile are shown in the chart in figure 3. [4]

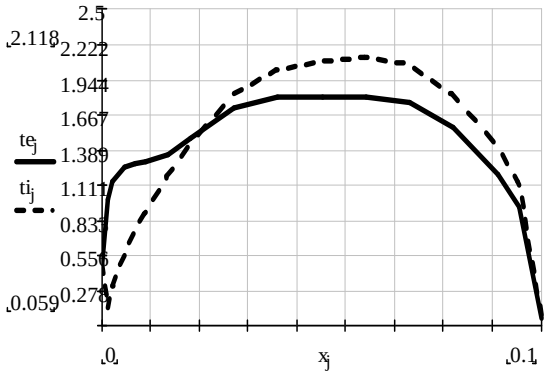

Fig. 3. Values of the transformation mapp functions

The flow around the profile study actually consists of studying the fluid flow around the conformal transformation circle. Conformal transformation preserves the Γ circulation.

The complex potential function describing the motion around the **K** circle is the following:

$$f_1(z) = -w_0\left[ze^{i\alpha} - \frac{a^2}{ze^{i\alpha}}\right] - \frac{i\Gamma}{2\pi}\cdot\ln z \qquad (3)$$

with $z \in C$; $z = x + iy$; or:

$$z = re^{i\theta} = r\left[\cos\theta + i\sin\theta\right] \qquad (4)$$

where r is the complex plane radius and θ is the complex plane point affix.

The complex potential describing the fluid emission motion through the trailing edge is:

$$f_2(z) = \frac{Q}{2\pi}\cdot\ln z \qquad (5)$$

$$Q = \frac{Q'}{b} \qquad (6)$$

where Q is the basic source outflow, and Q' is the total slit outflow.

The complex potential of the overall motion *f(z)* is calculated using the following ratio:

$$f(z) = f_1(z) + f_2(z)$$

$$f(z) = -w_0\left[ze^{i\alpha} - \frac{a^2}{ze^{i\alpha}}\right] - \frac{i\Gamma}{2\pi}\cdot\ln z + \frac{Q}{2\pi}\cdot\ln z \qquad (7)$$

But:

$$f(z) = f(r,\theta) = \varphi(r,\theta) + i\psi(r,\theta) \qquad (8)$$

where $z = r\left[\cos\theta + i\sin\theta\right]$ is the trigonometric form of the complex number, $\varphi(r,\theta)$ is the speed potential function, and $\psi(r,\theta)$ is the flow function.

Relation (8) reveals that:

$$\varphi(r,\theta) = \mathrm{Re}\left[f(r,\theta) \right] \tag{9}$$

As the speed potential function $\varphi(r,\theta)$ is known, the radial $v_r(r,\theta)$ and tangential $v_\theta(r,\theta)$ speeds may be calculated:

$$v_r(r,\theta) = \frac{\partial \varphi(r,\theta)}{\partial r} = -w_0\left[r + \frac{a^2}{r} \right]\cos(\theta+\alpha) + \frac{Q}{2\pi r}\left[\frac{a}{r}\cos\theta + \frac{a^2}{r^2}\cos 2\theta + \frac{a^3}{r^3}\cos 3\theta + 1 \right] \tag{10}$$

$$v_\theta(r,\theta) = \frac{1}{r}\frac{\partial \varphi(r,\theta)}{\partial \theta} = w_0\left[r + \frac{a^2}{r^2} \right]\sin(\theta+\alpha) + \frac{\Gamma}{2\pi r} + \frac{Q}{2\pi r^2}\left[\sin\theta + \frac{a}{r}\sin 2\theta + \frac{a^2}{r^2}\sin 3\theta \right] \tag{11}$$

The resulting speed $v_K(r,\theta)$ is defined by the relation (12):

$$v_K(r,\theta) = \sqrt{v_r^2(r,\theta) + v_\theta^2(r,\theta)} \tag{12}$$

For the classical profile, the (10) and (11) relations may be determined using the assumption $Q = 0$. In this case, the circulation Γ is calculated by the relation (13):

$$\Gamma = \pi a w_0 \sin\alpha \tag{13}$$

For the fluid emission profile, the circulation Γ also considers the fluid emission speed:

$$\Gamma = \pi a w_0 \sin\alpha + \pi a \frac{Q}{A}\sin\beta \tag{14}$$

where A [m^2] is the area that the jet is emitted through, and β [grd] is the jet deviation angle from the profile chord direction, set by applying the impulse theorem on a control surface limited to the profile.

On the aerodynamic profile outline, the speed in a particular point becomes:

$$v_p = \frac{v_K(a,\theta)}{\frac{\mathrm{d}z}{\mathrm{d}\tau}} \tag{15}$$

Local speed on the upper side of normal wing (V_{eo}) and jet wing (V_{eq}) is shown in figure 4.

Figure 5 show the local speed on the lower side of normal wing (V_{io}) and jet wing (V_{iq}).

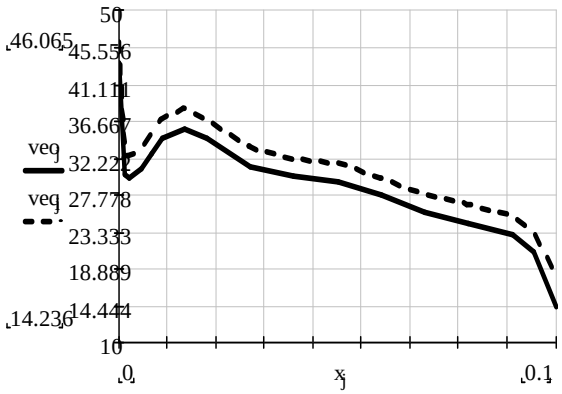

Fig. 4. Local speed distribution on upper side of wings

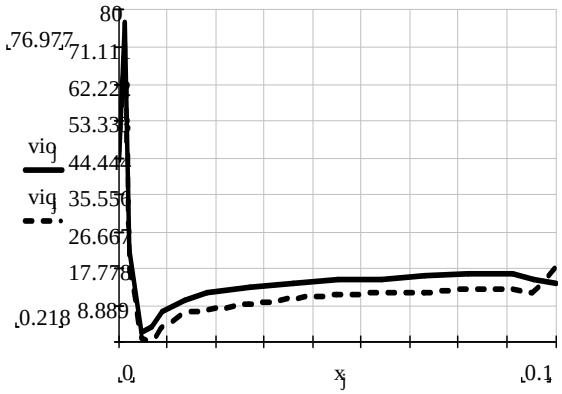

Fig. 5. Local speed distribution on lower side of wings

Knowing the speed v_p in any point on the profile outline, one may determine the expression of the pressure coefficient k_p in that point:

$$k_p = 1 - \frac{v_p^2}{w_0^2} \tag{16}$$

The local pressure p [N/m^2]:

$$p = p_0 + \frac{\rho}{2} k_p w_0^2 \tag{17}$$

is obtained using the pressure coefficient definition ratio:

$$k_p = \frac{p - p_0}{\frac{\rho}{2} w_0^2} \tag{18}$$

where p_0 [N/m^2] is the fluid flow pressure in a section undisturbed by the profile presence.

The pressure variation between two consecutive points on the profile outline is determined by the ratio:

$$\frac{dp}{dx};\ \frac{\Delta p}{\Delta x} = \frac{p_{i+1} - p_i}{x_{i+1} - x_i} \tag{19}$$

The pressure variation evolution was studied in both the classical (figures 6) and the fluid emission profiles (figures 7).

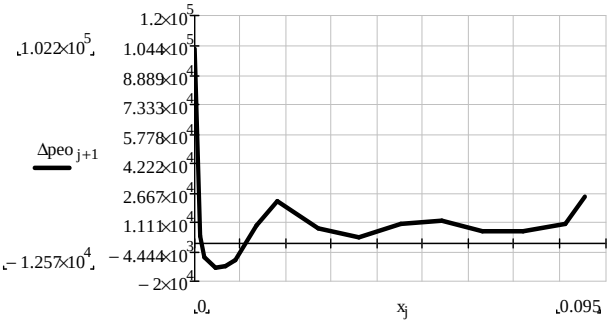

Fig. 6. Pressure variation evolution for classical profile

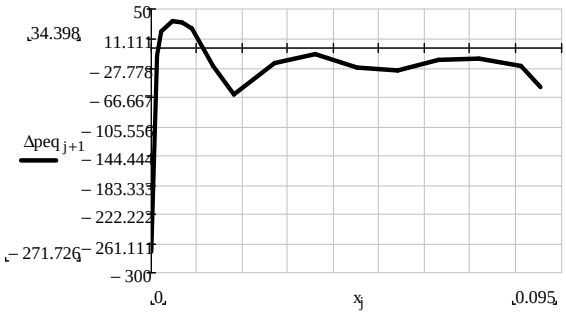

Fig. 7. Pressure variation evolution for fluid emission profile

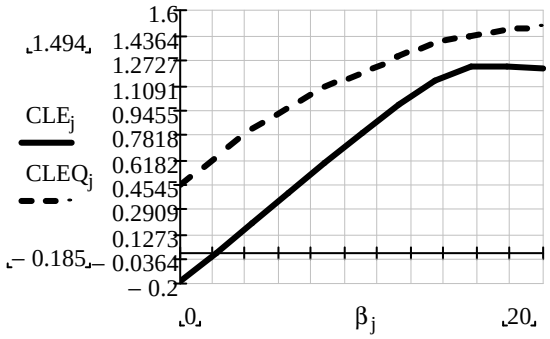

Fig. 8. Experimental lift force coefficient

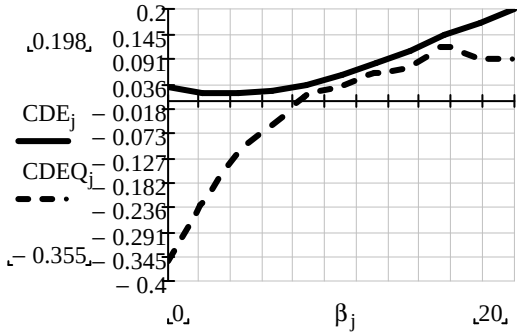

Fig. 9. Experimental drag force coefficient

The experimental tries was made on the wind tunnel from the "Fluid's Mechanics" Laboratory at the Technical University "Gheorghe Asachi" from Iasi. In the experience room it was created a speed $W_\infty = 20$ m/s, for the general current of fluid. Corresponding to this speed, the number of Reynolds is $Re = 1{,}3 \cdot 10^5$.

The measuring balance allows the determination of both the lift force and the drag force for a domain of incident angles $\beta = \pm 45°$. The incident angles "β" for which was made the experimental determinations has the following values: 0°; 2°; 4°; 6°; 8°; 10°; 12°; 14°; 16°; 18°; 20°; 22°.

There is no boundary layer detachment when the pressure variation is negative. If, however, the pressure variation is positive, a boundary layer detachment phenomenon occurs between the two point's x_i and x_{i+1}.

The input data considered when drafting the pressure variation evolution diagrams were:

$$\alpha = 8^o;\ W_0 = 20\ m/s;\ b = 0{,}5\ m;\ c = 0{,}1\ m$$
$$Q' = 3.10^{-4}\ m^3/s;\ A = 5.10^{-5}\ m^2.$$

4. CONCLUSIONS

For the input data considered, we noticed a better behavior, from the boundary layer detachment viewpoint, of the fluid emission profile as compared to the classical profile.

Fluid emission and boundary layer detachment on trailing edge area have an important effect on lift and drag forces. These influences are presented in figures 8 and 9.

Chart 8 presents the variation of the experimental lift force coefficient CLE for the blade without fluid emission and of the coefficient CLEQ for the fluid emission blade. The fluid emission determines the increase of the lift force coefficient.

Chart 9 presents the variation of the drag force coefficient CDE for the foil without fluid emission and of the coefficient CDEQ for the fluid emission blade.

The fluid emission determines the decrease of the drag force coefficient. In the field of the setting angles $\beta \in [0{,}10°]$, the resistance coefficient has negative values, which leads to some propulsion characteristics for the wing.

5. REFERENCES

1. Hepperle, Martin: (1988) *Neue Profile für Nurflügelmodelle*, FMT-Kolleg 8, Verlag für Technik und Handwerk, Baden-Baden, Germany.

2. Unverfehrt, Hans-Jürgen: (1990) *Faszination Nurflügel*, Verlag für Technik und Handwerk, Baden-Baden, Germany.

3. Hepperle, Martin: (1991) *Neue Profile für Elektro-Pylonmodelle*, FMT-Kolleg 10, Verlag für Technik und Handwerk, Baden-Baden, Germany.

4. Hepperle, Martin: (1986) *Neue Profile für Pylon und Speed*, FMT 6, Verlag für Technik und Handwerk, Baden-Baden.

5. Jakob, Otto: (1985) *Eppler 220 und Eppler 221*, FMT 2, Verlag für Technik und Handwerk, Baden-Baden.

Received: 23 January 2010 / Accepted: 10 May 2010 / Abstract published online: 18 May 2010